[Supplementary information]

Automation-assisted human skin-on-a-chip for modeling ultraviolet-induced injury and evaluation of photoprotective and regenerative modalities

Yu-Jeong Lee[a], Jieun Lee[b], Yoojin Na[b], Hoon Suk Rho[b], Min-Kyu Kang[a], YongTae Kim[*b], and Jeong-Kee Yoon[*a]

[a]Department of Systems Biotechnology, Chung-Ang University, Anseong-Si, Gyeonggi-Do, 17546, Republic of Korea.
[b]Mepsgen Co. Ltd, Seoul, Republic of Korea.

Email: jyoon342@cau.ac.kr (J. -K. Yoon) and ytkim@mepsgen.com (Y. Kim)

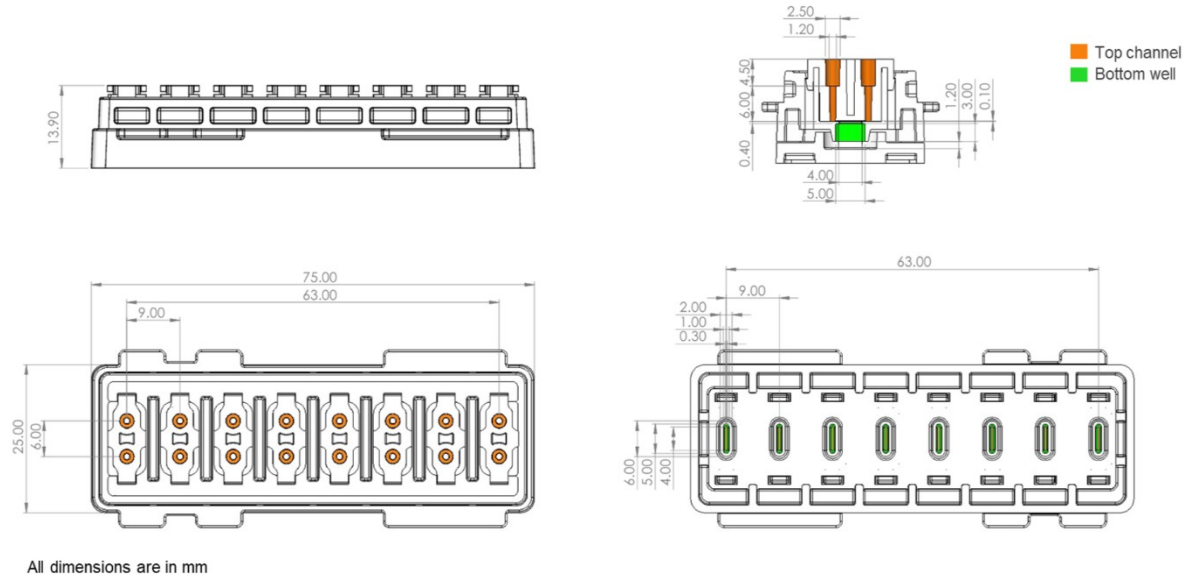

Figure S1. Dimensioned engineering drawings of the MEPS-TBC-WL device.
Top, side, and cross-sectional views are shown to illustrate the overall device footprint, 8-unit layout, and relative positions of the apical top channel (orange) and basolateral bottom well (green). Per unit, the total accessible volume of the apical channel compartment was 60 µL, consisting of approximately 20 µL in each inlet and outlet reservoir and approximately 20 µL in the channel region extending from the narrow connecting channel to the membrane-overlying area. The basolateral microwell had a working volume of 15 µL.

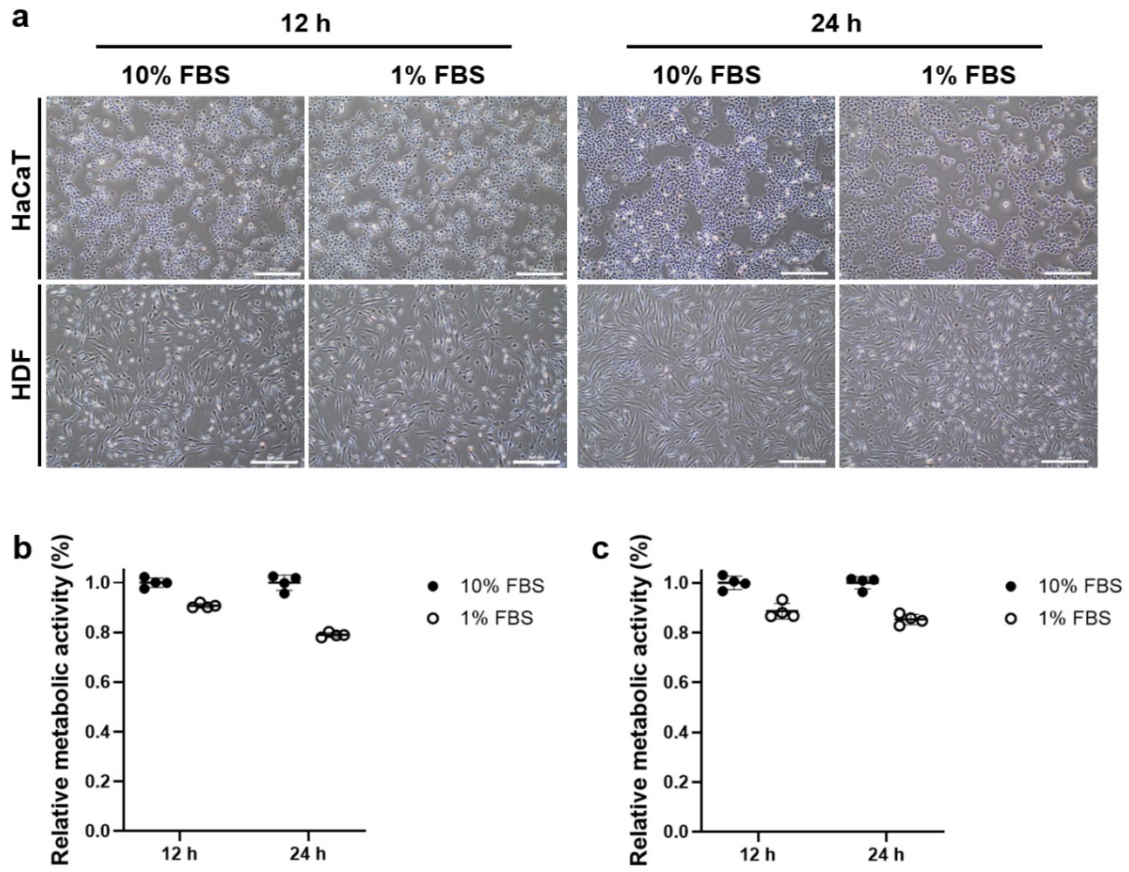

Figure S2. Validation of the low-serum pretreatment condition in HaCaTs and HDFs.
(a) Representative brightfield images of HaCaTs and HDFs after incubation in 10% FBS or 1% FBS for 12 h or 24 h. (b) Relative metabolic activity of HaCaTs under the indicated conditions, measured by CCK assay. (c) Relative metabolic activity of HDFs under the indicated conditions, measured by CCK assay. Short-term low-serum exposure reduced relative metabolic activity compared with 10% FBS controls, with a greater effect after 24 h, while gross cellular morphology was largely preserved. Values were normalized to the corresponding 10% FBS control at each time point. Data are presented as mean ± SD.

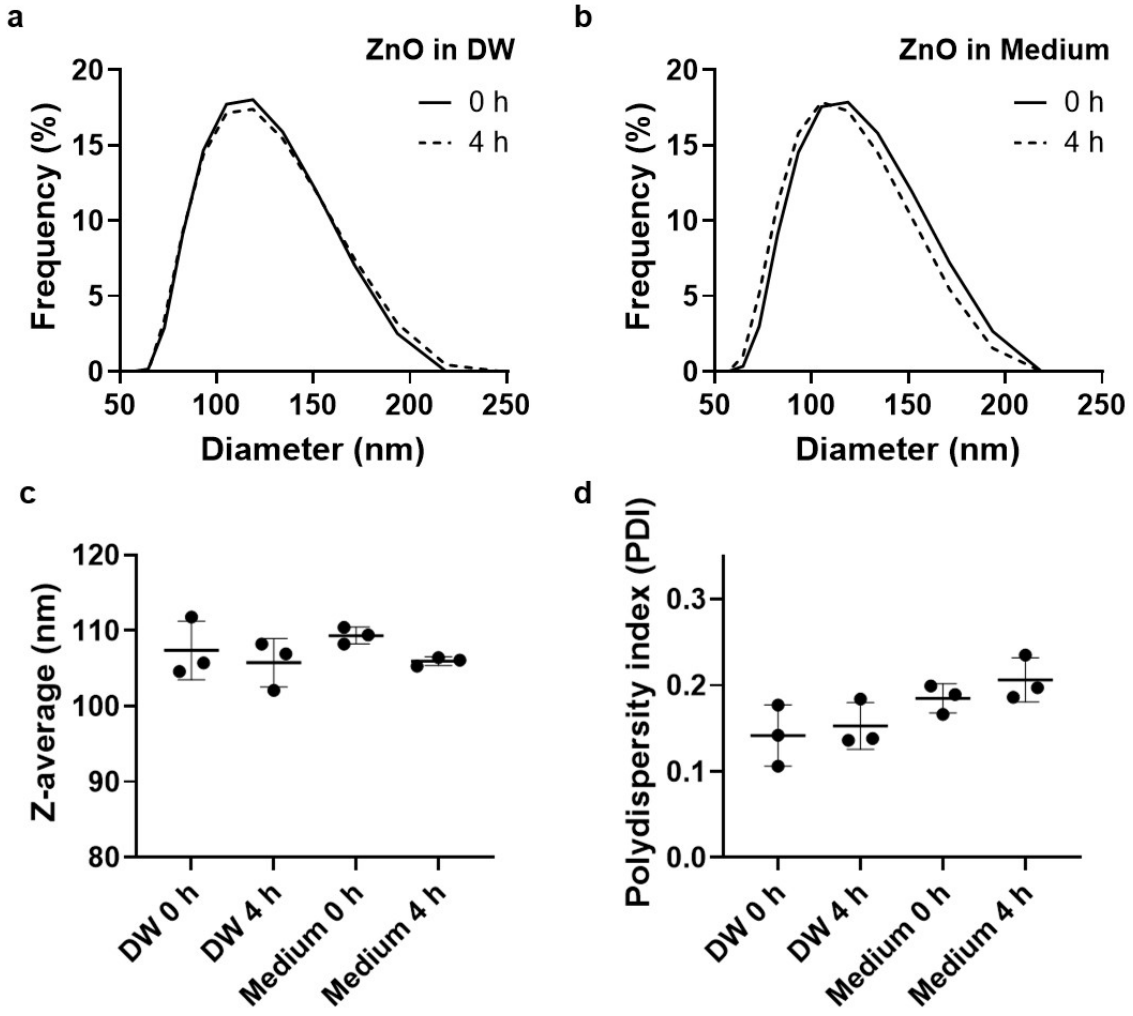

Figure S3. Dynamic light scattering (DLS) characterization of ZnO under relevant working conditions.

(a) Representative DLS size distribution curves of ZnO dispersions in deionized water (DW) immediately after preparation and after 4 h incubation. (b) Representative DLS size distribution curves of ZnO dispersions in 1% FBS-containing DMEM/F-12 immediately after preparation and after 4 h incubation. (c) Z-average hydrodynamic diameters of ZnO-containing samples under the indicated conditions. (d) Polydispersity index (PDI) values of ZnO-containing samples under the indicated conditions.

Condition	*Count rate (kCPS)*	*Z-average (nm)*	*PDI*
DW blank	0–1	ND	ND
Medium blank	0–1	ND	ND
ZnO in DW, 0 h	753 ± 49	107.4 ± 3.9	0.142 ± 0.036
ZnO in DW, 4 h	974 ± 80	105.7 ± 3.2	0.086 ± 0.085
ZnO in medium, 0 h	869 ± 43	109.3 ± 1.1	0.185 ± 0.017
ZnO in medium, 4 h	1037 ± 182	105.9 ± 0.6	0.206 ± 0.026

Table S1. Summary of DLS-derived count rate, Z-average hydrodynamic diameter, and polydispersity index (PDI) for ZnO dispersions under the indicated conditions.
Blank deionized water and blank 1% FBS-containing DMEM/F-12 controls yielded only near-background count rates (0–1 kCPS) without a reproducible particle peak; therefore, size statistics from blank runs were not interpreted. Data are presented as mean ± SD (n = 3). kCPS, kilo counts per second; ND, not determined.

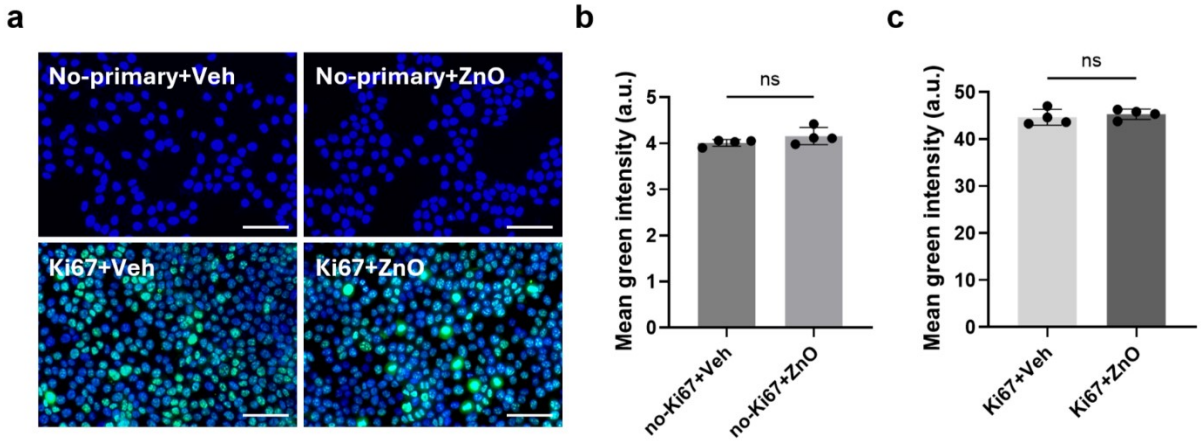

Figure S4. Control experiments excluding ZnO-related optical artefacts in Ki67 immunofluorescence imaging.
(a) Representative merged images of DAPI and green-channel signal from HaCaT samples processed either without Ki67 primary antibody (No-primary control) or with full Ki67 immunostaining under vehicle (Veh) or ZnO-treated conditions, using the same acquisition settings. (b) Quantification of mean green-channel intensity in the No-primary control samples. (c) Quantification of mean green-channel intensity in the corresponding Ki67-stained samples. Data are presented as mean ± SD; ns, not significant. Scale bars = 100 μm.

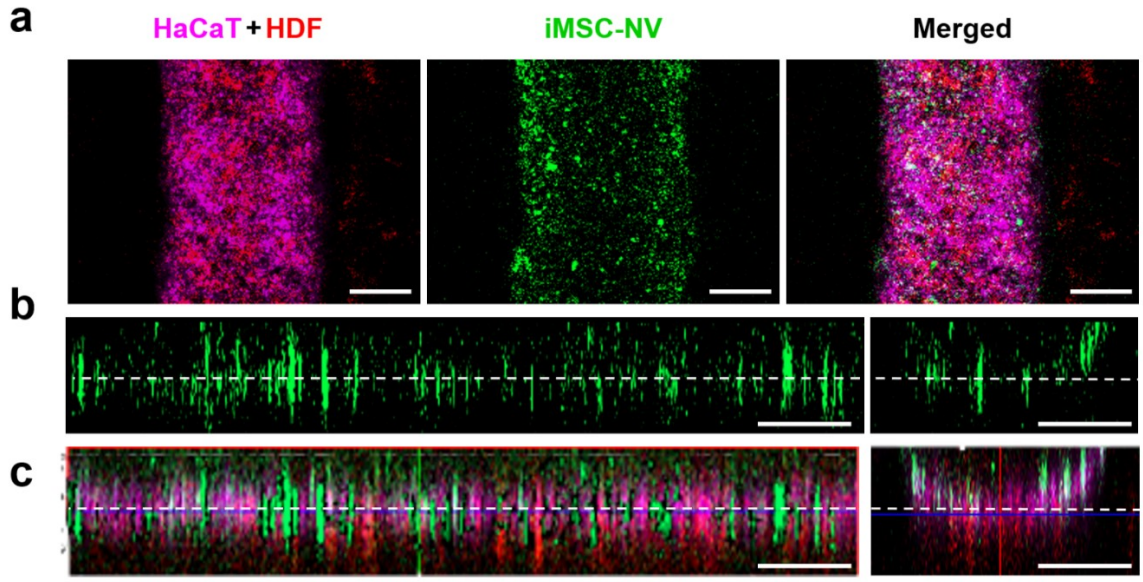

Figure S5. Split-channel and orthogonal views of the representative ROI shown in Fig. 4f.

(a) En face views of the same ROI showing the combined HaCaT/HDF channels (HaCaT, magenta; HDF, red), the iMSC-NV channel (green), and the merged image. (b) Orthogonal views of the iMSC-NV channel from the same ROI. (c) Corresponding orthogonal views of the merged image. Dashed white lines indicate the position of the porous membrane. Scale bars = 200 μm.